Auroral Disturbances as a Manifestation of Interplay Between Large-Scale and Mesoscale Structure of Magnetosphere-Ionosphere Electrodynamical Coupling

L. R. Lyons,[1] Y. Nishimura,[1] X. Xing,[1] Y. Shi,[1] M. Gkioulidou,[1] C.-P. Wang,[1] H.-J. Kim,[1] S. Zou,[2] V. Angelopoulos,[3] and E. Donovan[4]

Both slowly varying large-scale structure and a variety of disturbances occur within the coupled magnetosphere-ionosphere system along nightside plasma sheet magnetic field lines, and both are reflected in the aurora. Recently, there have been expansion and additions to radar systems, enhancements in ground auroral imaging, strategically placed multiple spacecraft of the Time History of Events and Macroscale Interactions during Substorms program, and new model development. Studies using these new capabilities are suggesting that much about the structure and disturbances along plasma sheet field lines may be understood based on a slowly changing large-scale structure describable by region 1 and 2 physics and its interplay with much more dynamic mesoscale structures associated with flow channels emanating from near the polar cap boundary. These new results also suggest a possible unifying view that many auroral disturbances (poleward boundary intensifications, streamers, substorms, and perhaps others) may be related to the mesoscale flow channels. If so, understanding the generation and propagation of the flow channels and their coupling with the large-scale background is critical. Evidence is now fairly strong that the flow channels consist of plasma with lower flux tube–integrated entropy than the surrounding plasma. Also, initial studies have led to the hypothesis that enhanced mesoscale flows from deep within the polar cap and impinging on the nightside polar cap boundary may be important for triggering the flow channels within the plasma sheet, the resulting highly structured flow of plasma into the plasma sheet, perhaps giving a highly structured source of plasma sheet plasma with highly variable properties, including entropy.

[1]Department of Atmospheric and Oceanic Sciences, University of California, Los Angeles, California, USA.

[2]Department of Atmospheric, Oceanic and Space Sciences, University of Michigan, Ann Arbor, Michigan, USA.

[3]Department of Earth and Space Sciences, University of California, Los Angeles, California, USA.

[4]Department of Physics and Astronomy, University of Calgary, Calgary, Alberta, Canada.

Auroral Phenomenology and Magnetospheric Processes: Earth and Other Planets
Geophysical Monograph Series 197

10.1029/2011GM001152

1. INTRODUCTION

Many space weather disturbances are associated with temporal changes and spatial structuring of electric fields and associated currents along plasma sheet magnetic field lines. They can be visually identified via the aurora, which is a manifestation of the electrodynamical coupling between the magnetosphere and ionosphere. Under the slow-flow approximation (neglect of the inertial term in the momentum equation) [*Wolf*, 1983], the electrodynamical coupling arises because magnetospheric particle magnetic drift can drive currents across closed magnetic field lines that are not divergence free when there are pressure gradients [*Heinemann*, 1999; *Lyons et al.*, 2009a]. For current continuity to be

maintained within the magnetosphere, this divergence leads to magnetic field-aligned currents (FACs) flowing to and from the ionosphere. FACs can also be driven when there are large spatial and/or temporal changes in particle velocity so that the inertial term cannot be neglected. Ionospheric electric fields adjust to give a divergence of the horizontal ionospheric currents that balances the FAC, giving current continuity in the ionosphere as well as the magnetosphere. Differences between the mapping along magnetic field lines of ionospheric electric fields to the magnetosphere and the magnetospheric electric field are mitigated by Alfven waves [*Southwood and Kivelson*, 1991; *Vogt et al.*, 1999; *Yoshikawa et al.*, 2011]. This leads to electrodynamic feedback between the magnetosphere and ionosphere that leads, under the slow variation assumption [*Wolf*, 1983], to identically mapped electric fields within both regions (except in localized regions of substantial field-aligned electric potential drops). Thus, while coupling with the solar wind is important for determining the overall strength of magnetospheric convection, it does not impose a distribution of electric fields within the ionosphere or magnetosphere. Instead, electrodynamical coupling controls this distribution.

Significant advances in understanding the coupled magnetosphere-ionosphere electrodynamic system are now starting to occur as a result of major improvements in our observational and modeling capabilities. Most important to the discussion here are ground-based radars, most of which have been deployed by the National Science Foundation, the continental-scale, high-resolution all-sky auroral imager (ASI) array [*Mende et al.*, 2008] and the multiple spacecraft constellation of NASA's Time History of Events and Macroscale Interactions during Substorms (THEMIS) program [*Angelopoulos*, 2008], and the Rice Convection Model (RCM) [*Harel et al.*, 1981; *Wolf et al.*, 2007]. Initial studies from these facilities and the RCM have suggested that much about the plasma sheet processes leading to space weather disturbances can be viewed as interplay *between a slowly changing large-scale structure and much more dynamic mesoscale structures* associated with flow channels. In addition, recent analyses have revealed the unexpected possibility that flow structure formed within the polar cap regions of open field lines (which, within the ionosphere, lies poleward of the auroral oval) may be important for driving the plasma sheet mesoscale structures.

In this chapter, we describe the pieces that are starting to emerge of the framework for understanding the dynamics and disturbances along plasma sheet field lines, including the large-scale structure and the mesoscale flow structures and disturbances associated with the flow channels. The possible connection with polar cap convection structure is also addressed.

2. LARGE-SCALE STRUCTURE

The properties of a slowly evolving (~tens of minutes to hours) large-scale structure, extending throughout the nightside plasma sheet and auroral oval, have been studied extensively with the RCM [*Erickson et al.*, 1991; *Jaggi and Wolf*, 1973; *Toffoletto et al.*, 2003; *Wang et al.*, 2004; *Wolf et al.*, 2007; *Gkioulidou et al.*, 2009]. The RCM evaluates the drift transport physics of plasma sheet particles and self-consistently includes the electrodynamic coupling with the ionosphere under a time-dependent magnetic field and variable rate of driving by the solar wind.

An example of the response to enhanced driving by the solar wind as simulated with the RCM [*Gkioulidou et al.*, 2009] is shown within the ionosphere in Figure 1. The two rows show FACs as mapped to the ionosphere and height-integrated Pedersen conductivity in the ionosphere as a function of magnetic latitude (Λ) and magnetic local time (MLT) within 3 h of midnight. Equipotentials are overlaid in each panel. An enhancement of solar wind driving was simulated by increasing the cross polar cap potential drop ($\Delta\Phi_{PCP}$) from 30 to 100 kV just after $T = 0$. At $T = 0$, immediately prior to the increase in $\Delta\Phi_{PCP}$, the model shows that the inner plasma sheet pressure [see *Gkioulidou et al.*, 2009] leads to weak FACs, referred to as region 2 (R2) currents, which are upward at midnight to dawn MLTs and downward at dusk to midnight MLTs and which map to the ionosphere at Λ ~66°–67°. Electrodynamic coupling between the plasma sheet and the ionosphere associated with these currents leads to strong shielding of electric fields from the region equatorward of the plasma sheet precipitation. Shielding is seen as a bending of equipotential contours away from midnight. This gives enhanced poleward-directed electric fields on the premidnight side (close together equipotentials) equatorward of the inner edge of the electron plasma sheet (identified from the equatorward edge of the height-integrated ionospheric Pedersen conductivity). These fields give strong plasma flows and are referred to as subauroral polarization (SAPS) electric fields. These lie in the region of downward R2 currents and are driven by gradients of the strongest inner magnetosphere ion pressures and low conductance in the subauroral ionosphere.

The SAPS electric field can be seen to move equatorward within the ionosphere along with the electron plasma sheet after the increase in $\Delta\Phi_{PCP}$. The $\Delta\Phi_{PCP}$ increase also leads to a gradual increase in plasma sheet pressures, pressure gradients, and R2 currents. Initially, enhanced electric fields penetrate equatorward of the plasma sheet, but shielding gradually reestablishes. The plasma sheet pressures and equipotentials within the equatorial plane well after the increase in $\Delta\Phi_{PCP}$ are illustrated in Figure 2. Plasma and magnetic field properties of this large-scale system have been verified

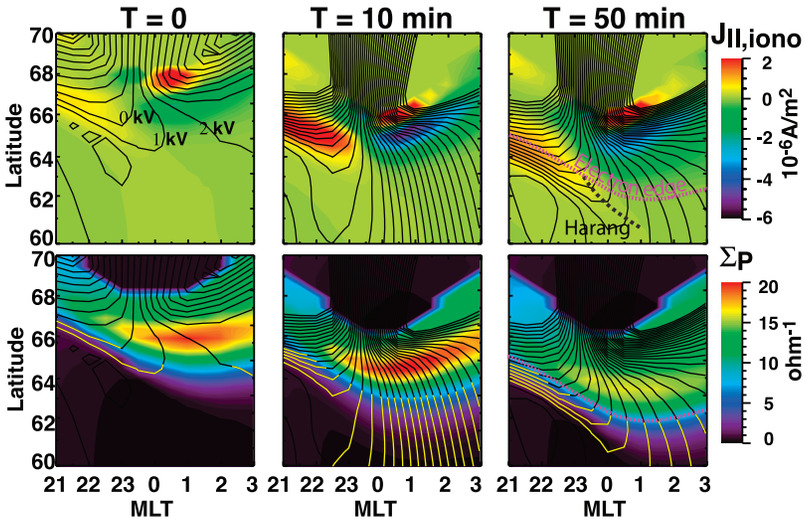

Figure 1. Rice Convection Model (RCM) results within the ionosphere using the Tsyganenko 1996 magnetic field model. Plasma boundary conditions were taken from a statistical analysis of 11 years of Geotail observations for weakly northward interplanetary magnetic field conditions [*Wang et al.*, 2007]. Results are shown just prior to the enhancement in convection ($T = 0$) and for indicated times after the enhancement. Field-aligned currents (FACs) are positive downward. Height-integrated Pederson conductivity in the bottom row reflects the energy flux of plasma sheet electron precipitation. Equipotentials are overlaid in each panel. Dashed lines in the panels for $T = 50$ min identify the Harang reversal [*Gkioulidou et al.*, 2009].

with observations from in situ spacecraft [e.g., *Wang et al.*, 2011, and references therein] and from radar observations from the ground [e.g., *Bristow and Jensen*, 2007; *Bristow et al.*, 2001; *Hughes and Bristow*, 2003; *Lyons et al.*, 2009b; *Zou et al.*, 2009a], demonstrating the importance of the magnetosphere-ionosphere electrical coupling in determining the large-scale particle, current, and electric field structure along plasma sheet field lines.

3. INTERPLAY BETWEEN LARGE-SCALE AND MESOSCALE STRUCTURE

Superposed on the large-scale ionospheric and plasma sheet flow structure are mesoscale perturbations [*Angelopoulos et al.*, 1992] that often have a substantially larger magnitude than the background. These bursts of flow within the plasma sheet are typically localized in the y direction [*Angelopoulos et al.*,

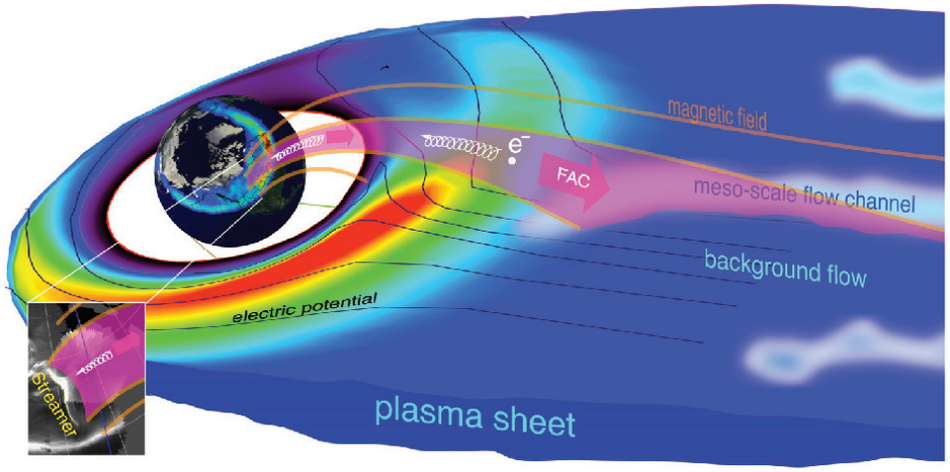

Figure 2. Coupling along magnetic field lines between plasma sheet particles near the equatorial plane and flows and the auroral ionosphere. Plasma pressures and electric potentials of the large-scale background obtained from the RCM well after the increase in $\Delta\Phi_{PCP}$ are shown in the equatorial plane, and the connection between mesoscale flow channels and auroral upward FAC and streamers is illustrated.

1996], so that they can be viewed as channels of earthward flow within the plasma sheet that are superposed on the large-scale pattern as sketched in Figure 2, and they are associated with transport of plasma perpendicular to the magnetic field direction.

The flow channels cause auroral activity that is also localized in longitude. Specifically, poleward boundary intensifications (PBIs) have been related to flow channels that can carry plasma across the nightside separatrix into the plasma sheet [*de la Beaujardière et al.*, 1994; *Lyons et al.*, 1999]. This can be seen in Figure 3, which shows a global auroral image from the Wideband Imaging Camera on the IMAGE spacecraft, with flow vector observations from the global SuperDARN radar array overlaid on the auroral image. This example is shown because of the two bright PBIs (that reach the yellow on the color scale and can be seen at geomagnetic latitude Λ ~73° on the nightside) and the quite good coverage of radar echoes over the polar cap and auroral oval. Following the format of *Zou et al.* [2009b], two types of ionospheric flow vectors are shown: the solid squares with thicker lines give flow vectors merged from multiple line-of-sight (LOS) velocity observations when they are available and the dots with thinner lines give the LOS velocities when only one such measurement is available at a given location. Note the two longitudinally localized regions of enhanced flow, identified in Figure 3 by solid white arrows, which appear to move from the polar cap into the plasma sheet adjacent to the two PBIs. The PBIs are to the right of the flow direction, as required for the converging Pedersen currents on the edges of the flow regions to give the upward FAC that are associated with discrete aurora.

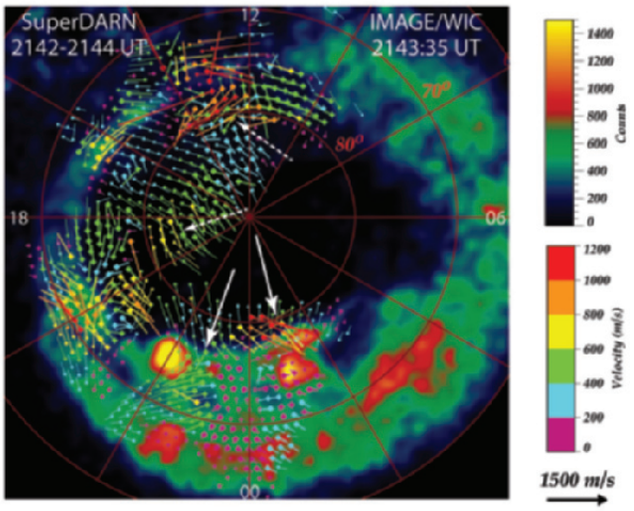

Figure 3. Global auroral image from the Wideband Imaging Camera on the IMAGE spacecraft, with flow vector observations from the global SuperDARN radar array overlaid on the auroral image. Two bright poleward boundary intensifications (PBIs) can be seen at geomagnetic latitude Λ ~73° on the nightside. Solid squares with thicker lines give flow vectors merged from line-of-sight (LOS) velocity observations when they are available, and the dots with thinner lines give the LOS velocities when only one such measurement is available at a given location. Solid white arrows identify two longitudinally localized regions of enhanced, polar cap flow associated with the PBIs, and dashed white arrows identify two additional localized polar cap flow enhancements.

Some PBIs develop into equatorward-moving auroral arcs that are roughly north-south oriented and are referred to as streamers. Streamers have been related to channels of enhanced earthward flows [*Rostoker et al.*, 1987; *Sergeev et al.*, 1999, 2000; *Zesta et al.*, 2000; *Henderson et al.*, 2002; *Pitkänen et al.*, 2011], which can extend from deep within the plasma sheet to near its earthward edge. An example of a streamer observed from the THEMIS all-sky camera network of North America is shown in Figure 4, and LOS flow speeds from the SuperDARN radars are overlaid on the aurora image. This example shows a streamer that extends in a southeastward direction from the poleward portion of the auroral oval and then turns westward within the equatorward portion of the oval.

The magenta arrow in Figure 4 illustrates the plasma sheet flow channel that would be expected to be associated with such a streamer. Based on the shape of the streamer, the flow channel appears to be guided by the large-scale background flow, first flowing around the Harang reversal, and then flowing westward within the SAPS region. The radar LOS flows are consistent with this picture, the flows in the eastern Saskatoon (SAS) beams being toward the radar (positive speeds) at the higher latitudes with echoes (Λ ~66°–68°). At Λ ~64°–66°, the LOS flows from the SAS radar switch from being toward the radar in the eastern beams to away from the radar in the western beams, which is as expected from approximately westward flow across the radar field of view (FOV). Based on the LOS flows observed by the Prince George radar, this westward flow appears to have extended well westward approximately parallel to the aurora. Images and flows before the time shown in Figure 4 show that the aurora shape and the LOS flows evolved with time together. This suggests that the flow channels affect the large-scale pattern in addition to being partially guided by the large-scale pattern, thus indicating that the full flow pattern may be viewable as an interplay between the large-scale and mesoscale structures.

PBIs and streamers are space weather disturbances that frequently occur, and the streamer association with mesoscale flow channels and FACs that couple between the plasma sheet and ionosphere is illustrated in Figure 2. The obvious question arises as to why the flow channels move rapidly

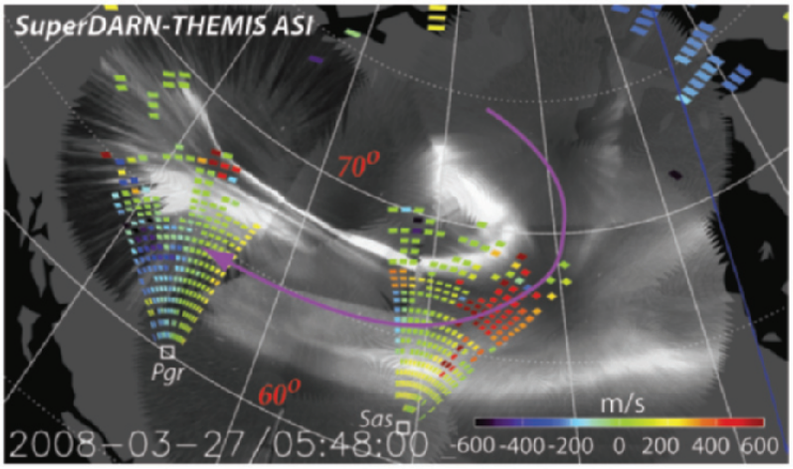

Figure 4. A streamer observed from the Time History of Events and Macroscale Interactions during Substorms (THEMIS) all-sky cameras, with LOS flow speeds from the SuperDARN radars overlaid on the aurora image as color-coded dots. The magenta arrow illustrates the plasma sheet flow channel that would be expected to be associated with the streamer seen in the auroral image.

earthward through the more slowly flowing background plasma sheet. It has been proposed that this motion occurs when there is a longitudinally localized region of plasma within flux tubes that has substantially reduced $P\mathcal{V}^{5/3}$ than the surrounding plasma, causing the reduced $P\mathcal{V}^{5/3}$ plasma to move earthward via interchange motion [*Chen and Wolf*, 1993; *Pontius and Wolf*, 1990; *Yang et al.*, 2008; *Zhang et al.*, 2009]. Here P is plasma pressure and $\mathcal{V}$ is flux tube volume. This proposal for the flow channels has been supported quite well by observations. In particular, the field lines within the flow channels are expected to be more dipolar than the surrounding field, and statistical analyses of observations have shown that is a common feature of flow channels [*Angelopoulos et al.*, 1994; *Dubyagin et al.*, 2010; *Ohtani et al.*, 2004]. Furthermore, *Dubyagin et al.* [2010] have shown that the dipolarization within flow channels occurs together with a reduction in $P\mathcal{V}^{5/3}$.

An example showing the connection between flow channels and streamers on 27 February 2009 is shown in Figure 5. Two combined images from four THEMIS ASI stations over central Canada are shown at the top, the blue line showing the magnetic midnight meridian. Two auroral streamers are identified. The first, labeled streamer 1 in the two panels, became discernible in the images ~1 min earlier than the time (07:53:00 UT) of the first panel. The second, labeled streamer 2 in the 07:54:36 panel, formed ~1.5 min after and ~1 h in MLT to the east of streamer 1. Mappings to the auroral oval of two of the THEMIS spacecraft, C and D, are overlaid on the images (as obtained with the Tsyganenko 1996 magnetic field model) [*Tsyganenko*, 1995]. The mappings show C being just to the east of streamer 1 and D being near the longitude of streamer 2. While azimuthal errors in the mapping can be as much as ~0.5 h in MLT [*Xing et al.*, 2010], C and D, located in the near-Earth plasma sheet at $X_{GSM} = -17$ and -11 R_E, respectively, appear to have been in good positions to measure the plasma associated with streamers 1 and 2, respectively.

The remainder of Figure 5 shows observations from C and D for a 17 min interval that includes the time of the two streamers, as described in the figure caption. Flow channels can clearly be seen at C at a time appropriate for the development of streamer 1 and at D for the development of streamer 2. C also saw two subsequent flow channels at times that are appropriate for subsequent streamers that were seen to have formed near the longitude of C in images subsequent to those shown in Figure 5. All of these flow channels show the characteristic features expected for earthward-moving channels of plasma having lower global entropy $P\mathcal{V}^{5/3}$ than was seen previously by the spacecraft. There are abrupt and substantial increases in B_z, which implies a corresponding decrease in $\mathcal{V}$, and simultaneous decreases in P_{tot}, which reflects an equatorial plasma pressure decrease. There are also simultaneous bursts of earthward flow, which is seen in both $\mathbf{V}_{perp}$ and $\mathbf{V}_{ExB}$. Consistency between $\mathbf{V}_{perp}$ and $\mathbf{V}_{ExB}$ demonstrates the accuracy of the calculated velocities and that the earthward flow is due to the electric drift, as is expected from interchange motion. The abrupt B_z and plasma parameter changes seen for flow channels, such as associated with streamers 1 and 2 in Figure 5, have led them to be referred to as "dipolarization fronts" [*Nakamura et al.*, 2001; *Runov et al.*, 2009]. *Runov et al.* [2009] noted the important feature that they appear to move earthward as coherent

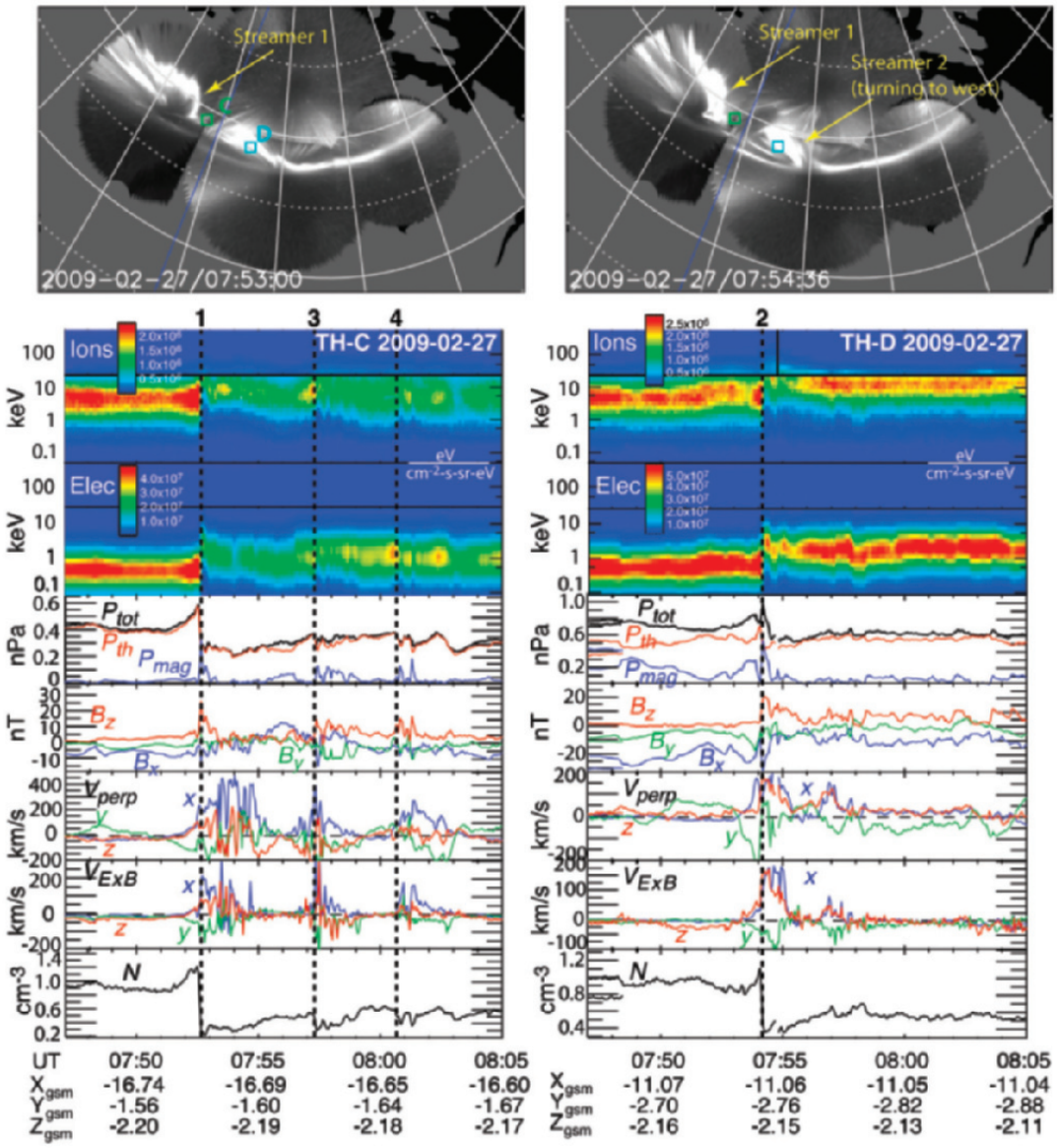

Figure 5. (top) Two combined images from four THEMIS all-sky auroral imager (ASI) stations over central Canada from 27 February 2009. The blue line gives the magnetic midnight meridian, and small squares give the mappings of THEMIS C and D to the auroral oval. (bottom) Observations from THEMIS C and D versus UT for 17 min including the times of the ASI images above. The top two panels show energy flux spectrograms for ions and electrons from the electrostatic analyzer [*McFadden et al.*, 2008] and solid-state detector. The next panels show from top to bottom the pressure (total P_{tot} as defined by *Xing et al.* [2009], thermal P_{th}, and magnetic P_{mag} from the THEMIS magnetometer [*Auster et al.*, 2008]), the GSM components of the magnetic field (B_x, B_y, and B_z), the components of the perpendicular velocity moment $\mathbf{V}_{perp}$, the components of the electric drift velocity $\mathbf{V}_{ExB}$ obtained from the measured electric [*Bonnell et al.*, 2008] and magnetic fields, and the plasma density N.

structures within the $x \sim -10$ to -20 R_E region of the plasma sheet, and the basic features of the large, abrupt dipolarization front events identified by *Runov et al.* [2009] appear to be the same for other flow channel events, such as those in the earlier studies referred to above.

4. INTERPLAY ASSOCIATED WITH SUBSTORM PREONSET SEQUENCE

The above discussion shows evidence that PBIs and streamers are related to mesoscale channels of earthward-flowing,

reduced entropy plasma and suggests that interplay with the large-scale field and plasma system is critical in determining the dynamics on both scales. This interplay becomes particularly interesting for substorms. While most PBIs and streamers are not associated with substorms, they are commonly seen as localized structures during the much larger-scale auroral displays of a substorm expansion phase [*Henderson et al.*, 1998]. Also, they have recently been found to often be a crucial part of the sequence of events that leads to substorm onset [*Nishimura et al.*, 2010a, 2010b], and this finding has been supported by the observations of preonset flow channels within the ionosphere [*Lyons et al.*, 2010a] and the plasma sheet [*Angelopoulos et al.*, 2008; *Lyons et al.*, 2010b; *Xing et al.*, 2010].

The auroral and flow pattern inferred to lead to substorm onset is illustrated in Figure 6. *Nishimura et al.* [2010b] observed that the auroral forms leading to substorm onset frequently approach the onset location from the east or northeast, consistent with the motion of the streamer and adjacent flow channels approximately following the dusk-side convection cell, leading to premidnight onsets as illustrated in Figure 6. Some streamers were observed to move in a pattern that followed the dawn convection cell, such motion generally leading to onsets located from near midnight to postmidnight as is also illustrated in Figure 6. These observations indicate the importance of the large-scale flow pattern in guiding the trajectory of the flow channels and their reduced entropy plasma. The importance of the large-scale pattern was supported by a high probability of Harang aurora, an auroral form having features that move with a pattern that mimics the convection flow around the Harang reversal.

These observations indicate that the large-scale convection pattern has a strong effect on the motion of the preonset auroral forms, and they suggest that the preonset flow channels bring reduced entropy plasma into the near-Earth plasma sheet, leading to onset via an instability that develops as a result of modification of plasma and magnetic field conditions caused by the intruding new plasma of the flow channel. It seems clear that flow channels must penetrate to the near-Earth plasma sheet to lead to a substorm onset, yet most streamers reaching the near-Earth plasma sheet do not lead to an onset. We thus have also investigated differences between auroral streamers reaching the near-Earth plasma sheet that do and do not lead to substorm expansion onset [*Nishimura et al.*, 2011]. While the two types of streamers were found to have similar characteristics, streamers that do not lead to onset were seen to lead to small intensification of a thin growth phase arc, and when an onset-related streamer was observed to reach the equatorward portion of the auroral oval, the preexisting, thin growth phase arc was much brighter than at the times of nononset-related streamers. The onset arc is typically near the poleward boundary of a diffuse growth-phase auroral band [*Samson et al.*, 1992], which is likely SAPS region proton aurora. These observations suggest that substorm onset instability is possible only when the preexisting inner plasma sheet pressure and pressure gradient is sufficiently large, which reflects the large-scale plasma distribution, but can be set up by a preceding mesoscale flow channel.

5. POSSIBLE RELATION TO MESOSCALE, POLAR CAP STRUCTURE

As discussed above, the mesoscale flow channels appear to play a crucial role in the dynamics and disturbances of the coupled magnetosphere-ionosphere system. If this is the case, it becomes important to understand the source of these flow channels and why the plasma within the flow channels has reduced $PV^{5/3}$. A potentially critical clue is the observation that flow enhancements leading to PBIs can cross into the

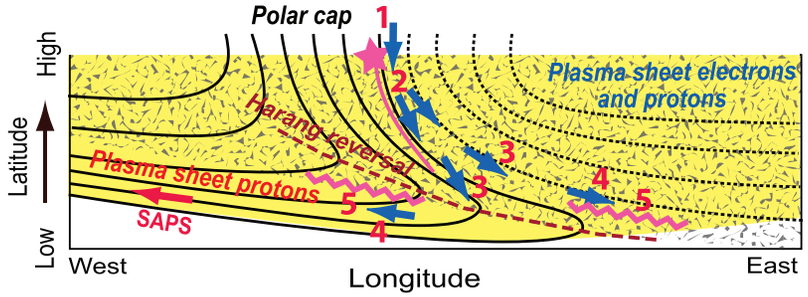

Figure 6. Schematic illustration of motion of preonset auroral forms and their relation to nightside ionospheric convection. The pink star, equatorward extending pink line, and azimuthally extended wavy lines indicate a PBI, an auroral streamer, and onset arcs, respectively. Blue arrows illustrate the plasma flow pattern inferred from preonset auroral motion. Numbers 1–5 show the time evolution of preonset aurora, and yellow and gray areas correspond to proton and electron precipitations. From the work of *Nishimura et al.* [2010b].

auroral oval from the high-latitude region of open polar cap magnetic fields [*de la Beaujardière et al.*, 1994; *Lyons et al.*, 2010b]. Flow crossing into the auroral oval from the polar cap is included in the illustration of Figure 6. It can also be seen in Figure 3, where the strong south-eastward-directed flows heading toward the western edge of the PBI near 01 MLT can be seen extending poleward of the poleward boundary of the aurora to $\Lambda > 80°$. Further supporting this possibility, *Nishimura et al.* [2010a] found several narrow flow bursts moving from far within the nightside polar cap and leading to PBIs that are followed by streamers, including one that led to a near-Earth substorm onset. This association leads to the hypothesis that enhanced mesoscale flows formed along polar cap field lines may contribute to the triggering of the mesoscale earthward flows along plasma sheet field lines that lead to PBIs, streamers, and substorm onset. Polar cap convection is often viewed as having a slowly varying large-scale structure. However, recent radar observations from within the polar cap are showing that the polar cap flows include significant mesoscale flow structures as does the plasma sheet [*Nishimura et al.*, 2010a; *Lyons et al.*, 2011]. This can also be seen in Figure 3, where two localized regions of enhanced flow are identified by dashed arrows in addition to the two localized flow enhancements associated with the nightside PBIs.

The connection between mesoscale flows formed within the polar cap and the triggering of the mesoscale earthward flows that lead to PBIs and streamers is seen clearly in the observations in Figure 7 (based on the work of *Lyons et al.* [2011]). Figure 7 shows LOS flow vectors measured within the polar cap from all beams of the PolarDARN radar (polar cap radar of the SuperDARN network) at Rankin Inlet and the new incoherent scatter radar at Resolute Bay (RISR). The flows are overlaid over a merger of the auroral images from three THEMIS ASIs located equatorward of the flow measurements. A time sequence of selected overlays is shown for the period leading up to a substorm onset at 06:26:30 UT on 21 September 2009. For this event, a flow enhancement is first seen deep within the polar cap in the westward- and poleward-looking beams of RISR, as indicated by the orange arrow in the 06:12:00 UT panel. These flows are directed southeastward,

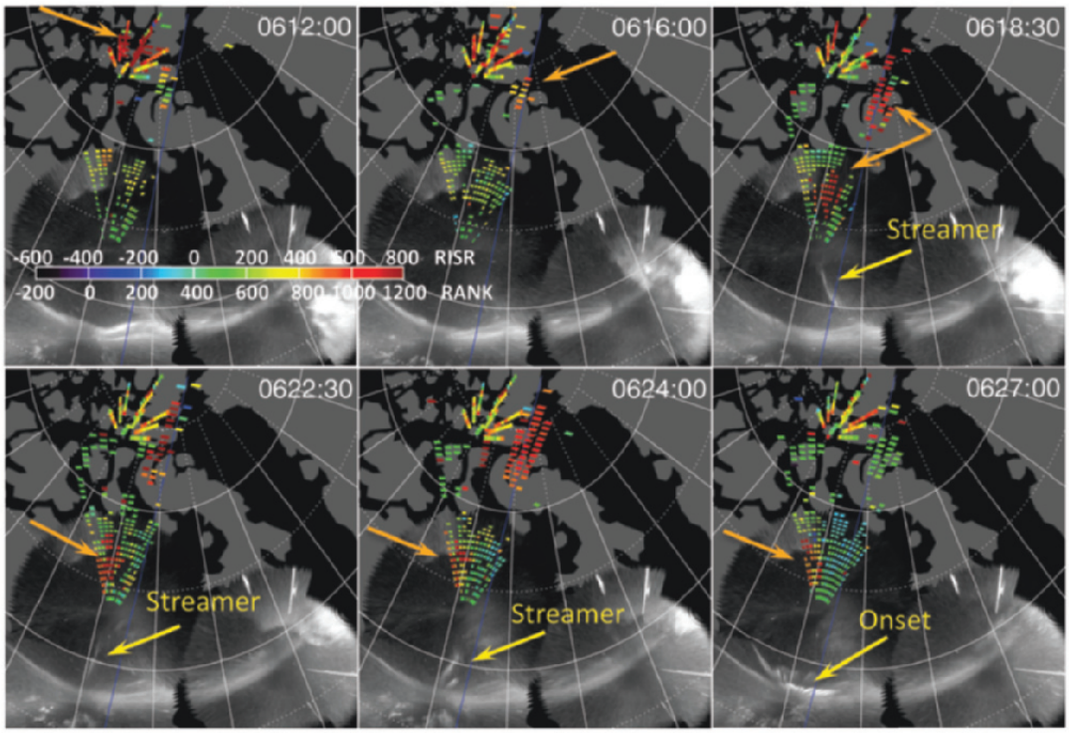

Figure 7. LOS flow vectors measured by the Rankin Inlet PolarDARN radar and Resolute Bay incoherent scatter radar (RISR) overlaid over a merger of the auroral images from three THEMIS ASIs located equatorward of the flow measurements. A time sequence of selected overlays is shown for the period leading up to a substorm onset 06:26:30 UT on 21 September 2009. The RISR and PolarDARN flows, available with 3 and 1 min resolution, respectively, that are overlaid in each panel are from the measurement interval with center time nearest the image time. Yellow arrows identify aurora features discussed in the text, and orange arrows identify equatorward-directed LOS flow channels. The blue line identifies magnetic midnight.

based on RISR flow vectors inferred from the los flows. Then, as indicated in the 06:16 UT panel, an equatorward-directed LOS flow enhancement is seen in the highest latitude echoes of the eastern PolarDARN beams. A longitudinally limited band of equatorward flows are then soon seen (06:18:30 UT panel) centered slightly to the east of the center of the PolarDARN FOV from Λ ~74° to 79°, and this channel of enhanced flow appears to be directly connected to an auroral streamer that is seen extending from Λ ~72° toward the diffuse auroral band lying near the equatorward boundary of the auroral oval. The enhanced flow channel then moved westward within the PolarDARN FOV, and the streamer moved westward along with the flow channel. This westward motion can be seen by comparing the 06:18:30 and 06:22:30 UT panels. The auroral substorm onset is then seen in the 06:27:00 UT panel very near the longitude of the flow enhancement and extending from the streamer longitude (identified in the 06:24:00 UT panel) to about 1 h in MLT to the east.

The flow channel that appears to lead to the streamer and to the substorm onset is narrow in longitudinal extent, much narrower than expected for large-scale convection, and is seen persistently for the 10 min period prior to onset from Λ ~78° to the most equatorward PolarDARN range gate at Λ = 74°. It is tempting to connect this flow channel to the flow enhancements seen earlier at higher latitudes by PolarDARN and RISR-N, suggesting that the enhanced flow propagated from well within the polar cap. While it is not possible to reliably determine if there was a connection to the flows seen at Λ >80° using the available LOS flow measurements, the connection of the flow channel seen at Λ <80° to the streamer and the ensuing onset seems quite clear.

6. SUMMARY

We have summarized evidence that has led us to suggest that the plasma sheet can be viewed as having a large-scale background state, which can be understood using models such as the RCM that include the energy-dependent magnetic drift and electrodynamic coupling with the ionosphere, and mesoscale flow channels, which can lead to disturbances, such as PBIs, streamers, and substorms. Interplay between the large-scale background and the flow channels partially guides the trajectory of the flow channels and plays an important role in controlling the occurrence and features of ensuing disturbances. Also, the interplay with the flow channels affects the large-scale pattern.

We illustrate this framework using the combination of THEMIS ASI images of the aurora in Figure 8 from an unusually

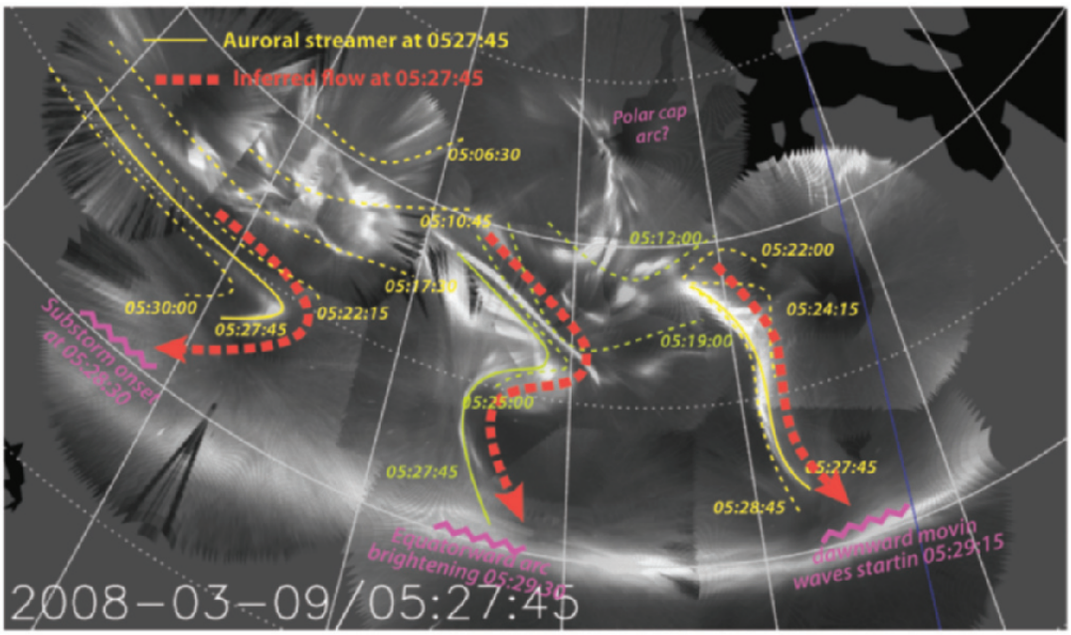

Figure 8. Auroral image at 05:27:45 UT on 9 March 2009 from the THEMIS ASIs, with north to the top. Magnetic latitude circles are drawn as solid lines at 60° and 70°, and longitude lines are drawn at 1 h magnetic local time intervals. The blue line identifies magnetic midnight. Three auroral streamers are identified, the solid yellow curves identifying the streamers at the time of the image, and the dashed yellow curves giving the streamer locations in preceding and subsequent images with the times identified. Red dashed arrows illustrate the flow channels that would be expected to be associated with the streamers at 05:27:45 UT.

clear, disturbed night over North America. The considerable activity seen within the poleward portion of the auroral oval is, we propose, associated with reduced total entropy flow channels. Several auroral streamers are seen simultaneously in the image. Based on our proposed framework, the streamers are like weather fronts, separating plasma masses of different properties. Here they separate higher entropy plasma from lower entropy plasma that is being brought closer to the Earth within the flow channels from the outer plasma sheet boundary. These "fronts" lie along the edge of flow regions (the edge to the right of the flow direction) where upward FAC are associated with discrete aurora, and they slowly move through the background plasma as weather fronts do through the atmosphere. Three streamers (i.e., fronts) are identified in Figure 8, where the solid curves identified the streamers at the time of the image (05:27:45 UT), and the dashed curves show the motion of the fronts as indicated by the streamer locations in preceding and subsequent images. Red dashed arrow illustrates the plasma sheet flow channels that we estimate to have been associated with the streamers at 05:27:45 UT.

Our suggested partial guiding of the inferred flow channels by the large-scale flow can be seen by the streamers at and after the time of the image. The westernmost channel follows the shape of the evening side flow contours, moving first equatorward and dawnward, and then around the Harang electric field reversal to the duskside broad region of diffuse aurora that characterizes the SAPS region [*Zou et al.*, 2009b]. On the other hand, the easternmost flow channel reaches the SAPS region near magnetic midnight and is deflected dawnward as is the dawnside large-scale flow pattern. Each of these flow channels leads to a different type of auroral disturbance when it reaches near the equatorward auroral boundary, as indicated. The results suggest a unifying view that substorms, PBIs, streamers, and other disturbances may be all related to mesoscale flow channels, which come from the distant plasma sheet and couple with the more slowly varying large-scale background. If so, understanding the generation and propagation of these mesoscale flow channels and the coupling with the large-scale background is critical for understanding space weather disturbances.

We have also discussed measurements that have led to the hypothesis that enhanced mesoscale flows from deep within the open polar cap region and impinging on and crossing the nightside polar cap boundary may be important for the triggering of the mesoscale earthward flows along plasma sheet field lines that lead to PBIs, streamers, and substorm onset. The resulting highly structured flow of plasma into the plasma sheet should give a highly structured source of plasma for the plasma sheet, so that the properties of the entering plasma should be quite variable. This could give plasma with reduced global entropy ($PV^{5/3}$) along some of the entering flow channels, allowing these channels to propagate earthward within the plasma sheet (equatorward with the ionosphere) toward the equatorward portion of the plasma sheet. We have not addressed how mesoscale flow structures may form within the polar cap, but it appears plausible that they should connect to the dayside so that spatial and temporal variations of dayside reconnection could be a possible source of the polar cap structure.

Acknowledgments. This review brings together aspects from several projects at UCLA, which were supported by a number of different grants. These include National Science Foundation grants ATM-0646233 and AGS-1042255 (Lyons, Nishimura), NASA grants NNX09AI06G (Xing), NNX09AQ41H (Gkioulidou), NNX07AF66G (Wang), NNX06AB89G (Kim), and NNX10AL30G (Shi), and NASA contract NAS5-02099 (Angelopoulos). The research at the University of Michigan was supported by NSF AGS1111476 (Zou). We thank S. Mende and H. Frey for the use of the THEMIS ASI and IMAGE WIC data and the CSA for logistical support in fielding and data retrieval from the GBO stations. We thank J. M. Ruohoniemi, N. Nishitani, and G. Sofko for access and support for the SuperDARN and PolarDARN data. We thank M. Nicolls and C. Heinselman for access and support of the RISR data.

REFERENCES

Angelopoulos, V. (2008), The THEMIS mission, *Space Sci. Rev.*, *141*(1–4), 5–34, doi:10.1007/s11214-008-9336-1.

Angelopoulos, V., W. Baumjohann, C. F. Kennel, F. V. Coroniti, M. G. Kivelson, R. Pellat, R. J. Walker, H. Lühr, and G. Paschmann (1992), Bursty bulk flows in the inner central plasma sheet, *J. Geophys. Res.*, *97*(A4), 4027–4039.

Angelopoulos, V., C. F. Kennel, F. V. Coroniti, R. Pellat, M. G. Kivelson, R. J. Walker, C. T. Russell, W. Baumjohann, W. C. Feldman, and J. T. Gosling (1994), Statistical characteristics of bursty bulk flow events, *J. Geophys. Res.*, *99*(A11), 21,257–21,280.

Angelopoulos, V., et al. (1996), Multipoint analysis of a bursty bulk flow event on April 11, 1985, *J. Geophys. Res.*, *101*(A3), 4967–4989.

Angelopoulos, V., et al. (2008), Tail reconnection triggering substorm onset, *Science*, *321*(5891), 931–935, doi:10.1126/science.1160495.

Auster, H. U., et al. (2008), The THEMIS fluxgate magnetometer, *Space Sci. Rev.*, *141*(1–4), 235–264, doi:10.1007/s11214-008-9365-9.

Bonnell, J. W., F. S. Mozer, G. T. Delory, A. J. Hull, R. E. Ergun, C. M. Cully, V. Angelopoulos, and P. R. Harvey (2008), The electric field instrument (EFI) for THEMIS, *Space Sci. Rev.*, *141*(1–4), 303–341, doi:10.1007/s11214-008-9469-2.

Bristow, W. A., and P. Jensen (2007), A superposed epoch study of SuperDARN convection observations during substorms, *J. Geophys. Res.*, *112*, A06232, doi:10.1029/2006JA012049.

Bristow, W. A., A. Otto, and D. Lummerzheim (2001), Substorm convection patterns observed by the Super Dual Auroral Radar Network, *J. Geophys. Res.*, *106*, 24,593–24,609.

Chen, C. X., and R. A. Wolf (1993), Interpretation of high-speed flows in the plasma sheet, *J. Geophys. Res.*, *98*(A12), 21,409–21,419.

de la Beaujardière, O., L. R. Lyons, J. M. Ruohoniemi, E. Friis-Christensen, C. Danielsen, F. J. Rich, and P. T. Newell (1994), Quiet-time intensifications along the poleward auroral boundary near midnight, *J. Geophys. Res.*, *99*(A1), 287–298.

Dubyagin, S., V. Sergeev, S. Apatenkov, V. Angelopoulos, R. Nakamura, J. McFadden, D. Larson, and J. Bonnell (2010), Pressure and entropy changes in the flow-braking region during magnetic field dipolarization, *J. Geophys. Res.*, *115*, A10225, doi:10.1029/2010JA015625.

Erickson, G. M., R. W. Spiro, and R. A. Wolf (1991), The physics of the Harang discontinuity, *J. Geophys. Res.*, *96*(A2), 1633–1645.

Gkioulidou, M., C.-P. Wang, L. R. Lyons, and R. A. Wolf (2009), Formation of the Harang reversal and its dependence on plasma sheet conditions: Rice Convection Model simulations, *J. Geophys. Res.*, *114*, A07204, doi:10.1029/2008JA013955.

Harel, M., R. A. Wolf, P. H. Reiff, R. W. Spiro, W. J. Burke, F. J. Rich, and M. Smiddy (1981), Quantitative simulation of a magnetospheric substorm, 1. Model logic and overview, *J. Geophys. Res.*, *86*(A4), 2217–2241.

Heinemann, M. (1999), Role of collisionless heat flux in magnetospheric convection, *J. Geophys. Res.*, *104*(A12), 28,397–28,410.

Henderson, M. G., G. D. Reeves, and J. S. Murphree (1998), Are north-south aligned auroral structures an ionospheric manifestation of bursty bulk flows?, *Geophys. Res. Lett.*, *25*(19), 3737–3740.

Henderson, M. G., L. Kepko, H. E. Spence, M. Connors, J. B. Sigwarth, L. A. Frank, and H. J. Singer (2002), The evolution of north-south aligned auroral forms into auroral torch structures: The generation of omega bands and ps6 pulsations via flow bursts, in *Sixth International Conference on Substorms*, edited by R. M. Winglee, pp. 169–174, The Univ. of Washington, Seattle.

Hughes, J. M., and W. A. Bristow (2003), SuperDARN observations of the Harang discontinuity during steady magnetospheric convection, *J. Geophys. Res.*, *108*(A5), 1185, doi:10.1029/2002JA009681.

Jaggi, R. K., and R. A. Wolf (1973), Self-consistent calculation of the motion of a sheet of ions in the magnetosphere, *J. Geophys. Res.*, *78*(16), 2852–2866.

Lyons, L. R., T. Nagai, G. T. Blanchard, J. C. Samson, T. Yamamoto, T. Mukai, A. Nishida, and S. Kokubun (1999), Association between Geotail plasma flows and auroral poleward boundary intensifications observed by CANOPUS photometers, *J. Geophys. Res.*, *104*(A3), 4485–4500.

Lyons, L. R., C. Wang, M. Gkioulidou, and S. Zou (2009a), Connections between plasma sheet transport, Region 2 currents, and entropy changes associated with convection, steady magnetospheric convection periods, and substorms, *J. Geophys. Res.*, *114*, A00D01, doi:10.1029/2008JA013743.

Lyons, L. R., S. Zou, C. Heinselman, M. Nicolls, and P. Anderson (2009b), Poker flat radar observations of the magnetosphere-ionosphere coupling electrodynamics of the earthward penetrating plasma sheet following convection enhancements, *J. Atmos. Sol. Terr. Phys.*, *71*(6–7), 717–728, doi:10.1016/j.jastp.2008.09.025.

Lyons, L. R., Y. Nishimura, Y. Shi, S. Zou, H.-J. Kim, V. Angelopoulos, C. Heinselman, M. J. Nicolls, and K.-H. Fornacon (2010a), Substorm triggering by new plasma intrusion: Incoherent-scatter radar observations, *J. Geophys. Res.*, *115*, A07223, doi:10.1029/2009JA015168.

Lyons, L. R., Y. Nishimura, X. Xing, V. Angelopoulos, S. Zou, D. Larson, J. McFadden, A. Runov, S. Mende, and K.-H. Fornacon (2010b), Enhanced transport across entire length of plasma sheet boundary field lines leading to substorm onset, *J. Geophys. Res.*, *115*, A00I07, doi:10.1029/2010JA015831.

Lyons, L. R., Y. Nishimura, H.-J. Kim, E. Donovan, V. Angelopoulos, G. Sofko, M. Nicolls, C. Heinselman, J. M. Ruohoniemi, and N. Nishitani (2011), Possible connection of polar cap flows to pre- and post-substorm onset PBIs and streamers, *J. Geophys. Res.*, *116*, A12225, doi:10.1029/2011JA016850.

McFadden, J. P., C. W. Carlson, D. Larson, M. Ludlam, R. Abiad, B. Elliott, P. Turin, M. Marckwordt, and V. Angelopoulos (2008), The THEMIS ESA plasma instrument and in-flight calibration, *Space Sci. Rev.*, *141*(1–4), 277–302, doi:10.1007/s11214-008-9440-2.

Mende, S. B., S. E. Harris, H. U. Frey, V. Angelopoulos, C. T. Russell, E. Donovan, B. Jackel, M. Greffen, and L. M. Peticolas (2008), The THEMIS array of ground-based observatories for the study of auroral substorms, *Space Sci. Rev.*, *141*(1–4), 357–387, doi:10.1007/s11214-008-9380-x.

Nakamura, R., W. Baumjohann, R. Schödel, M. Brittnacher, V. A. Sergeev, M. Kubyshkina, T. Mukai, and K. Liou (2001), Earthward flow bursts, auroral streamers, and small expansions, *J. Geophys. Res.*, *106*, 10,791–10,802.

Nishimura, Y., et al. (2010a), Preonset time sequence of auroral substorms: Coordinated observations by all-sky imagers, satellites, and radars, *J. Geophys. Res.*, *115*, A00I08, doi:10.1029/2010JA015832.

Nishimura, Y., L. Lyons, S. Zou, V. Angelopoulos, and S. Mende (2010b), Substorm triggering by new plasma intrusion: THEMIS all-sky imager observations, *J. Geophys. Res.*, *115*, A07222, doi:10.1029/2009JA015166.

Nishimura, Y., L. R. Lyons, V. Angelopoulos, T. Kikuchi, S. Zou, and S. B. Mende (2011), Relations between multiple auroral streamers, pre-onset thin arc formation, and substorm auroral onset, *J. Geophys. Res.*, *116*, A09214, doi:10.1029/2011JA016768.

Ohtani, S., M. A. Shay, and T. Mukai (2004), Temporal structure of the fast convective flow in the plasma sheet: Comparison between observations and two-fluid simulations, *J. Geophys. Res.*, *109*, A03210, doi:10.1029/2003JA010002.

Pitkänen, T., A. T. Aikio, O. Amm, K. Kauristie, H. Nilsson, and K. U. Kaila (2011), EISCAT-Cluster observations of quiet-time near-Earth magnetotail fast flows and their signatures in the ionosphere, *Ann. Geophys.*, *29*(2), 299–319, doi:10.5194/angeo-29-299-2011.

Pontius, D. H., Jr., and R. A. Wolf (1990), Transient flux tubes in the terrestrial magnetosphere, *Geophys. Res. Lett.*, *17*(1), 49–52.

Rostoker, G., A. T. Y. Lui, C. D. Anger, and J. S. Murphree (1987), North-south structures in the midnight sector auroras as viewed by the Viking imager, *Geophys. Res. Lett.*, *14*(4), 407–410.

Runov, A., V. Angelopoulos, M. I. Sitnov, V. A. Sergeev, J. Bonnell, J. P. McFadden, D. Larson, K.-H. Glassmeier, and U. Auster (2009), THEMIS observations of an earthward-propagating dipolarization front, *Geophys. Res. Lett.*, *36*, L14106, doi:10.1029/2009GL038980.

Samson, J. C., L. R. Lyons, P. T. Newell, F. Creutzberg, and B. Xu (1992), Proton aurora and substorm intensifications, *Geophys. Res. Lett.*, *19*(21), 2167–2170.

Sergeev, V. A., K. Liou, C.-I. Meng, P. T. Newell, M. Brittnacher, G. Parks, and G. D. Reeves (1999), Development of auroral streamers in association with localized impulsive injections to the inner magnetotail, *Geophys. Res. Lett.*, *26*(3), 417–420.

Sergeev, V. A., et al. (2000), Multiple-spacecraft observation of a narrow transient plasma jet in the Earth's plasma sheet, *Geophys. Res. Lett.*, *27*(6), 851–854.

Southwood, D. J., and M. G. Kivelson (1991), An approximate description of field-aligned currents in a planetary magnetic field, *J. Geophys. Res.*, *96*(A1), 67–75.

Toffoletto, F., S. Sazykin, R. Spiro, and R. Wolf (2003), Inner magnetospheric modeling with the Rice Convection Model, *Space Sci. Rev.*, *107*(1), 175–196.

Tsyganenko, N. A. (1995), Modeling the Earth's magnetospheric magnetic field confined within a realistic magnetopause, *J. Geophys. Res.*, *100*(A4), 5599–5612.

Vogt, J., G. Haerendel, and K. H. Glassmeier (1999), A model for the reflection of Alfvén waves at the source region of the Birkeland current system: The tau generator, *J. Geophys. Res.*, *104*(A1), 269–278.

Wang, C.-P., L. R. Lyons, M. W. Chen, and F. R. Toffoletto (2004), Modeling the transition of the inner plasma sheet from weak to enhanced convection, *J. Geophys. Res.*, *109*, A12202, doi:10.1029/2004JA010591.

Wang, C.-P., L. R. Lyons, T. Nagai, J. M. Weygand, and R. W. McEntire (2007), Sources, transport, and distributions of plasma sheet ions and electrons and dependences on interplanetary parameters under northward interplanetary magnetic field, *J. Geophys. Res.*, *112*, A10224, doi:10.1029/2007JA012522.

Wang, C.-P., M. Gkioulidou, L. R. Lyons, R. A. Wolf, V. Angelopoulos, T. Nagai, J. M. Weygand, and A. T. Y. Lui (2011), Spatial distributions of ions and electrons from the plasma sheet to the inner magnetosphere: Comparisons between THEMIS-Geotail statistical results and the Rice Convection Model, *J. Geophys. Res.*, *116*, A11216, doi:10.1029/2011JA016809.

Wolf, R. A. (1983), The quasi-static (slow-flow) region of the magnetosphere, in *Solar Terrestrial Physics*, edited by L. Carovillano and J. M. Forbes, pp. 303–368, D. Reidel, Dordrecht, Netherlands.

Wolf, R. A., R. W. Spiro, S. Sazykin, and F. R. Toffoletto (2007), How the Earth's inner magnetosphere works: An evolving picture, *J. Atmos. Sol. Terr. Phys.*, *69*(3), 288–302, doi:10.1016/j.jastp.2006.07.026.

Xing, X., L. R. Lyons, V. Angelopoulos, D. Larson, J. McFadden, C. Carlson, A. Runov, and U. Auster (2009), Azimuthal plasma pressure gradient in quiet time plasma sheet, *Geophys. Res. Lett.*, *36*, L14105, doi:10.1029/2009GL038881.

Xing, X., L. Lyons, Y. Nishimura, V. Angelopoulos, D. Larson, C. Carlson, J. Bonnell, and U. Auster (2010), Substorm onset by new plasma intrusion: THEMIS spacecraft observations, *J. Geophys. Res.*, *115*, A10246, doi:10.1029/2010JA015528.

Yang, J., F. R. Toffoletto, R. A. Wolf, S. Sazykin, R. W. Spiro, P. C. Brandt, M. G. Henderson, and H. U. Frey (2008), Rice Convection Model simulation of the 18 April 2002 sawtooth event and evidence for interchange instability, *J. Geophys. Res.*, *113*, A11214, doi:10.1029/2008JA013635.

Yoshikawa, A., O. Amm, H. Vanhamäki, and R. Fujii (2011), A self-consistent synthesis description of magnetosphere-ionosphere coupling and scale-dependent auroral process using shear Alfvén n wave, *J. Geophys. Res.*, *116*, A08218, doi:10.1029/2011JA016460.

Zesta, E., L. R. Lyons, and E. Donovan (2000), The auroral signature of earthward flow bursts observed in the magnetotail, *Geophys. Res. Lett.*, *27*(20), 3241–3244.

Zhang, J.-C., R. A. Wolf, R. W. Spiro, G. M. Erickson, S. Sazykin, F. R. Toffoletto, and J. Yang (2009), Rice Convection Model simulation of the substorm-associated injection of an observed plasma bubble into the inner magnetosphere: 2. Simulation results, *J. Geophys. Res.*, *114*, A08219, doi:10.1029/2009JA014131.

Zou, S., L. R. Lyons, M. J. Nicolls, C. J. Heinselman, and S. B. Mende (2009a), Nightside ionospheric electrodynamics associated with substorms: PFISR and THEMIS ASI observations, *J. Geophys. Res.*, *114*, A12301, doi:10.1029/2009JA014259.

Zou, S., L. R. Lyons, C.-P. Wang, A. Boudouridis, J. M. Ruohoniemi, P. C. Anderson, P. L. Dyson, and J. C. Devlin (2009b), On the coupling between the Harang reversal evolution and substorm dynamics: A synthesis of SuperDARN, DMSP, and IMAGE observations, *J. Geophys. Res.*, *114*, A01205, doi:10.1029/2008JA013449.

V. Angelopoulos, Department of Earth and Space Sciences, University of California, Los Angeles, CA 90095-1567, USA.

E. Donovan, Department of Physics and Astronomy, University of Calgary, 2500 University Drive, Calgary, Alberta T2N 1N4, Canada.

M. Gkioulidou, H.-J. Kim, L. R. Lyons, Y. Nishimura, Y. Shi, C.-P. Wang, and X. Xing, Department of Atmospheric and Oceanic Sciences, University of California, Los Angeles, CA 90095-1565, USA. (larry@atmos.ucla.edu).

S. Zou, Department of Atmospheric, Oceanic and Space Sciences, University of Michigan, Ann Arbor, MI 48109, USA.